Journal of Power Sources 196 (2011) 5138–5142

Contents lists available at ScienceDirect

Journal of Power Sources

journal homepage: www.elsevier.com/locate/jpowsour

Short communication

Large scale synthesis of nickel oxide/multiwalled carbon nanotube composites by direct thermal decomposition and their lithium storage properties

Chaohe Xu, Jing Sun*, Lian Gao*

The State Key Lab of High Performance Ceramics and Superfine Microstructure, Shanghai Institute of Ceramics, Chinese Academy of Sciences, 1295 Ding Xi Road, Shanghai 200050, China

ARTICLE INFO

Article history:
Received 22 October 2010
Received in revised form
22 December 2010
Accepted 1 February 2011

Keywords:
Nickel oxide
Carbon nanotube
Hybrid materials
Anode materials
Lithium ion batteries

ABSTRACT

A large scale direct thermal decomposition method has been developed to prepare NiO/MWCNT nanocomposites. The as-prepared NiO nanoparticles are uniformly coated onto the surface of MWCNTs. The well crystallized NiO/MWCNT composites show superior electrochemical performance in Li ion batteries. The lithium storage capacity maintains at ~800 mAh g^{-1} after 50 discharge/charge cycles, which is much larger than those reported for NiO and its composites. Therefore, the NiO/MWCNT composites have significant potentials for application in energy storage devices. The direct thermal decomposition method is a versatile route for preparing carbon nanotube-inorganic hybrid electrode materials for lithium ion batteries.

1. Introduction

Recently, there is great interest in controllable synthesis of carbon nanotubes (CNTs)-inorganic hybrid materials [1,2]. These composites have been widely developed as electrode materials for energy storage devices due to their durability, nontoxicity, cheapness, and in particular superior electrochemical properties [3–6]. The electrochemical performance of these composites could be greatly affected by the uniformity, surface areas and the maintenance of electrical contacts between CNTs and inorganic nanostructures [7]. Therefore, many efforts have been devoted to develop synthetic methods for preparing inorganic nanoparticles uniformly coated on the surface or loaded into the inner cavities of CNTs, such as MnO_2/CNTs [8,9], SnO_2/CNTs [10–12], Fe_3O_4/CNTs [13] and Cu_2O/CNTs [14]. Iron oxide/CNT composites have been synthesized and showed improved lithium storage properties and stable cyclic retention [15]. A simple solution method has been adopted to synthesize SnO_2/MWCNT composites that the SnO_2 nanoparticles coated onto the surface and filled into inner cavities of MWCNTs [16]. Though several methods have been applied to synthesize CNT-inorganic hybrid materials, the experimental procedure is complex or with low yield due to the low solubility of CNTs in common solvents. This is one of the critical factors restricting the commercial availability of the large-scale CNT-inorganic hybrid materials [17,18].

Owing to their superior properties, nickel oxide has been under extensive investigation as an important functional inorganic materials, such as fuel cell [19], solar cells [20,21], lithium ion batteries (LIBs) and supercapacitors [22–25]. Loosely packed NiO nanoflakes [26] and nanoplatelets [27] with porous structures have been obtained by facile chemical precipitation and hydrothermal method, which showed excellent electrochemical performance as electrode materials for supercapacitors and lithium ion batteries, respectively. NiO nanotubes with specific capacitance of 80.49 F g^{-1} have been synthesized through a precursor method [23]. NiO/Ni [28] and NiO/Ag [29] composites have been prepared as electrode materials for LIBs and showed excellent initial discharge specific capacities. However, the capacity loss was very large after several discharge/charge cycles and capacity retentions were less than 50% for such composites. Therefore, mesoporous carbon and carbon nanotubes have been introduced into the NiO/carbon-based electrode materials, for utilizing their larger surface areas, pore structures and superior electron transport properties. The solvothermal, hydrothermal and spray pyrolyzed methods have been applied to synthesize NiO/C nanocomposites, which showed enhanced capacity retention compared to pure NiO nanoparticles [30–33]. Kyotani et al. [34] investigated nickel oxide nanoribbons encapsulated into the cavity of the carbon nanotubes by metal organic chemical vapor deposition. Hollow nickel microspheres covered with oriented carbon nanotubes have been synthesized via

* Corresponding authors. Tel.: +86 21 52412718; fax: +86 21 52413122.
E-mail addresses: jingsun@mail.sic.ac.cn (J. Sun), liangao@mail.sic.ac.cn (L. Gao).

0378-7753/$ – see front matter © 2011 Elsevier B.V. All rights reserved.
doi:10.1016/j.jpowsour.2011.02.001

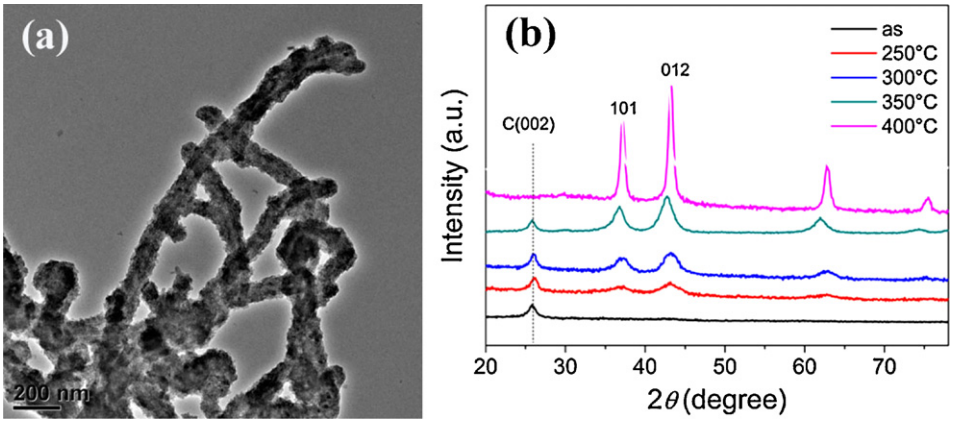

Fig. 1. (a) TEM image of the as prepared sample, (b) XRD curves of the NiO/MWCNT composites.

chemical vapor deposition at 800 °C [35]. And also, NiO nanoparticles have been loaded onto the surface of MWCNTs using sodium dodecyl sulfate (SDS) as a soft template or functionalized by benzenesulfonic [36,37] and showed enhanced electrochemical performance. However, NiO nanoparticles in NiO/MWCNT composites were usually aggregated together and nonuniformly coated onto the surface of MWCNT. Recently, the NiO nanofibers reinforced by SWCNTs have been prepared by electrospinning and exhibited a higher reversible capacity and lower capacity loss compared to pure NiO fibers, mainly because the three-dimensional electric network formed by CNTs provided large surface areas and contributed to high conductivity [38].

Recently, a facile method for the synthesis of metal oxide nanocrystals with controllable shape and size based on direct thermal decomposition of metal nitrates in octadecylamine have been developed by Li's group [39]. The method is rapid, economical and easily scaled up. Inspired by this, we developed the direct thermal decomposition procedure to prepare the NiO/MWCNT nanocomposites in N-methyl-2-pyrrolidone (NMP) solvent with high yield. NiO nanoparticles are uniformly coated on the surface of MWCNTs. The composites show enhanced lithium storage capacity compared with the reported results of NiO composites. The direct thermal decomposition method has great potential in synthesis of carbon nanotube-inorganic hybrid materials as electrode materials for LIBs.

2. Experimental

2.1. Materials synthesis

All chemicals were of analytical grade and used without further purification. MWCNTs were purchased from Chengdu Institute of Organic Chemistry, Chinese Academy of Sciences.

MWCNTs prepared by the catalytic decomposition of CH_4 were purified in the following process. First, 1.0 g of pristine MWCNTs was dried in a vacuum oven at 60 °C for 24 h. The dried samples were mixed with 45 ml concentrated nitric acid and sonicated for 30 min. Then, the suspensions were transferred into a 250 ml three-necked round-bottomed flask and refluxed at 140 °C for 6 h with magnetic stirring. The mixtures were separated through 0.22 μm member filter and washed with distilled water and absolute ethanol until the pH value reached neutral. Finally, the acid-treated MWCNTs were dried at 60 °C for 24 h in a vacuum oven.

Nickel oxide/MWCNT composites were synthesized by a two-step process. In a typical procedure, 500 mg acid-treated MWCNTs were mixed with 250 ml N-methyl-2-pyrrolidone (NMP) and sonicated for 120 min. A homogeneous suspension with MWCNT concentration of 2 mg mL^{-1} was formed. And then, 10 mmol $Ni(NO_3)_2{\cdot}6H_2O$ was poured into the above suspension and magnetically stirred for 60 min. Then, the suspensions were transferred into a 500 ml three-necked round-bottomed flask and refluxed at 180 °C in oil bath for 60 min with magnetic stirring. Subsequently, the flask was taken out and allowed to cool to room temperature naturally. The mixtures were separated through 0.22 μm member filter and washed with distilled water and absolute ethanol several times. The composites were dried in vacuum at 80 °C overnight. Finally, the as-prepared powders were annealed in a muffle furnace at different temperatures and kept for further use. The yield of the NiO/MWCNTs is about 1.0 g.

2.2. Characterization methods

Phase identification was performed on the powder X-ray diffraction pattern (XRD), using D/max 2550 V X-ray diffractionmeter with Cu-Kα irradiation at λ = 1.5406 Å. Transmission electron microscopy (TEM), High Resolution Transmission electron microscopy (HRTEM) and energy-dispersive X-ray spectroscopy (EDS) were performed on JEM-2100F Electron Microscope with an accelerating voltage of 200 kV. Field-emission scanning electron microscope (FE-SEM) was performed on JSM-6700F at an acceleration voltage of 10.0 kV.

2.3. Galvanostatic charge/discharge tests

The electrochemical properties of the NiO/MWCNT composites as a negative electrode used in Li-ion batteries were characterized at room temperature. The working electrode was made from the mixture of the active materials, acetylene black, and polyvinylidene fluoride (PVDF) binder in a weight ratio of 80:10:10. Li foil was used as the counter electrode. The electrolyte was 1 M $LiPF_6$ in a 50:50 w/w mixture of ethylene carbonate (EC) and dimethyl carbonate (DMC). Cell assembly was carried out in a glove box with the concentrations of moisture and oxygen below 1 ppm. The electrode activities were measured using a CT2001 battery tester. The cell was charged and discharged between 3.0 and 0.010 V with a current density of 50 mA g^{-1}.

3. Results and discussion

The TEM image of the as prepared sample is shown in Fig. 1(a). Amorphous nickel oxide nanoparticles are uniformly coated on the surface of MWCNTs as shown in the TEM image. The amorphous nature is demonstrated by the XRD curves as shown in Fig. 1(b), in which only one diffractive peak appears coincident with the

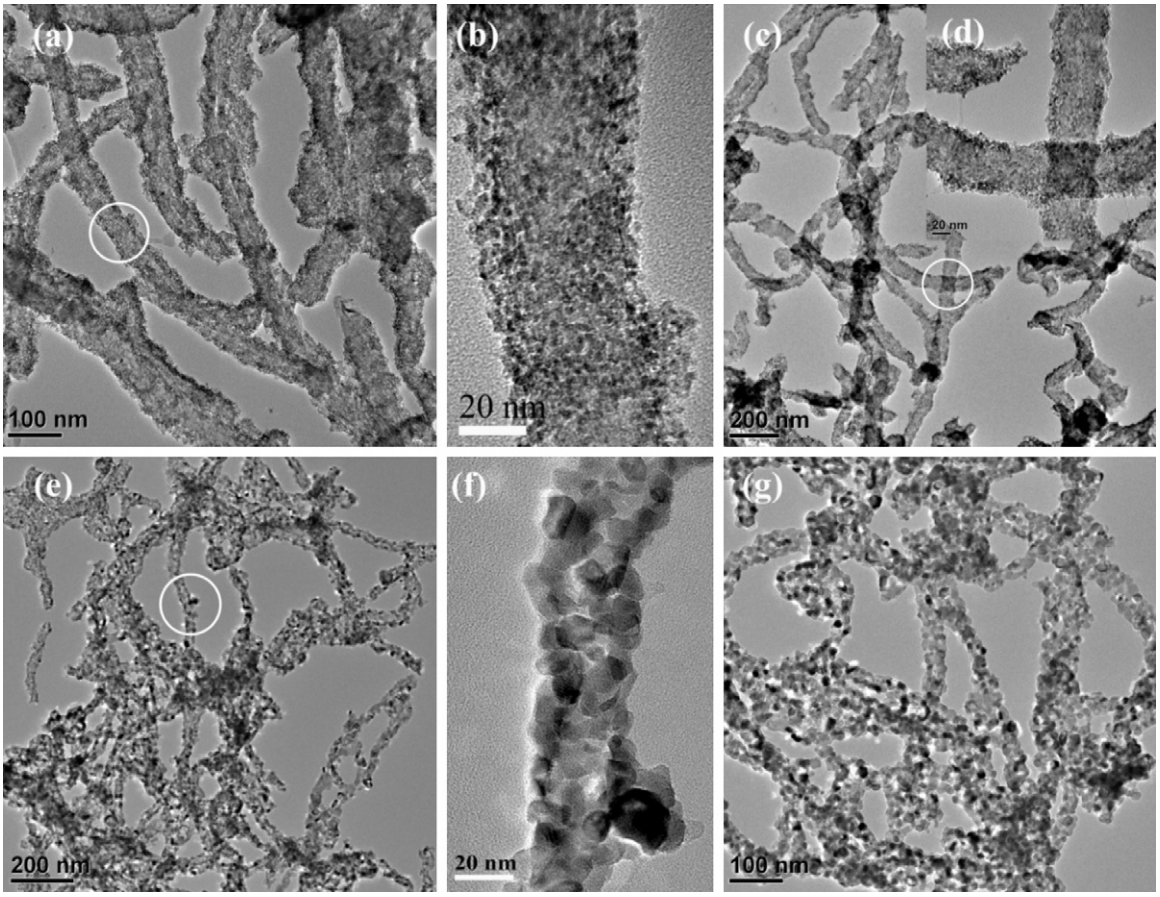

Fig. 2. TEM images of NiO/MWCNT composites, nanotubes and nanochains after annealed at different conditions (a–b) 250 °C/4 h; (c–d) 300 °C/1 h; (e–f) 350 °C/1 h; (g) 400 °C/1 h.

main peak of *h*-C(0 0 2) for carbon nanotubes. Fig. 2 shows the TEM images of the NiO/MWCNT composites after annealed under different temperatures. From Figs. 2(a–d) and 3, it can be seen that the NiO nanoparticles are uniformly coated on the surface of MWCNTs. The XRD patterns clearly show the (1 0 1), (0 1 2), (1 1 0) and (1 1 3) reflections of NiO (JCPDS card no. 44-1159; Fig. 1(b)). The broad peaks indicate that the crystallized NiO nanoparticles are very small. The particle size calculated by Scherrer equation is 3.4 and 3.8 nm for samples annealed at 250 and 300 °C, respectively. These are coincident well with the high magnification TEM image (Fig. 2(b and d)). After thermal treatment at 350 and 400 °C for 1 h, the XRD patterns clearly show the (1 0 1), (0 1 2), (1 1 0) and (1 1 3) reflections of NiO samples, and the *h*-C(0 0 2)reflection peak of carbon nanotube is weakened at 350 °C or disappeared completely at 400 °C. These coincide well with the results of TG test (Fig. 4). TG results show that the as prepared sample shows a total weight loss of 72.79% in the studied temperature range. Two distinct weight

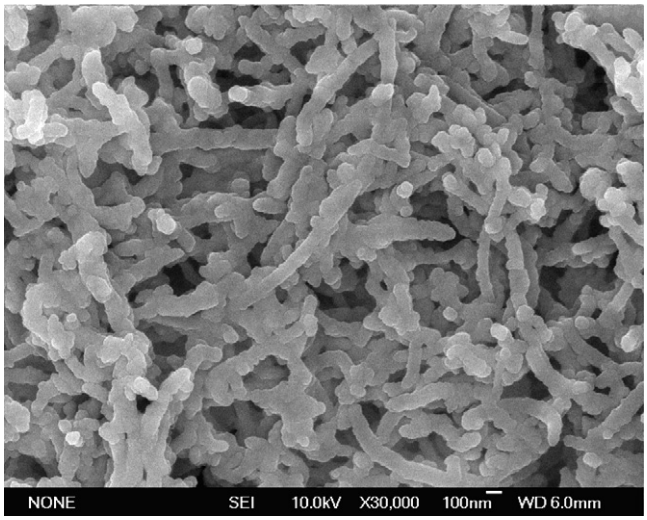

Fig. 3. SEM image of the NiO/MWCNT composites annealed at 300 °C for 1 h.

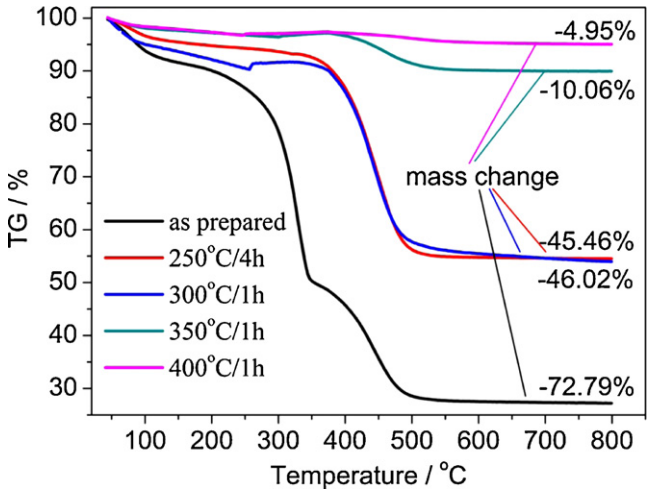

Fig. 4. Thermo gravimetric analysis showing the weight losses of sample synthesized at different conditions.

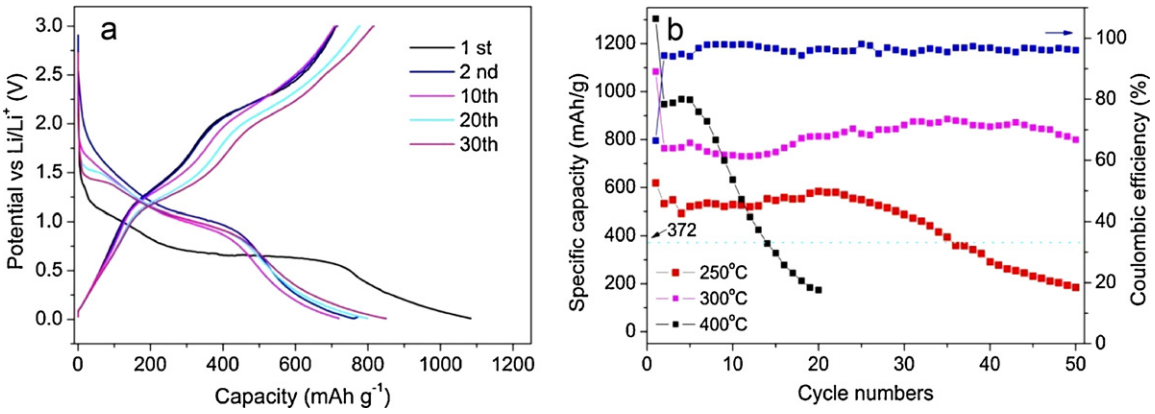

Fig. 5. (a) Discharge/charge curves of NiO/MWCNT composites annealed at 300 °C for 1 h; (b) the discharge/charge capacity profiles of NiO/MWCNT composites in 5 mV–3 V (vs. Li^+/Li) at a constant current density of 50 mA g^{-1}.

loss zones can be seen, a ~45% weight loss attributed to dehydration of the samples from 100 to 350 °C and a ~27.3% weight loss from 350 to 500 °C attributed to the decomposition of MWCNTs. For samples annealed at 250 or 300 °C, it has only one major zone of mass loss with a total loss about ~45.5% (the calculated yield of the as prepared sample is about 1.1 g based on the TG results). A total weight loss of ~10% or 5% occured for samples annealed at 350 or 400 °C should be mainly attributed to the dehydration and the burning of residual MWCNTs. Fig. 2(e–g) shows the TEM images of NiO/MWCNT composites and nanotubes after being annealed at 350 and 400 °C for 1 h. When the temperature increased to 350 °C, a tube structure was observed from Fig. 2(e). Fig. 2(f) shows the high magnification TEM image of the circular area in Fig. 2(e). It can be seen that the nanoparticles with size of 10–20 nm assembled into long tube structure. Further increasing the temperature to 400 °C, NiO nanotubes with particle size of 20–30 nm are obtained. The BET surface areas are 204.1, 139.9, 89.4 and 66.9 $m^2\ g^{-1}$ for samples calcinated at 250 °C/4 h, 300, 350 and 400 °C/1 h, respectively, while the BET surface area of MWCNTs is 107.7 $m^2\ g^{-1}$.

We chose the samples annealed at 250 and 300 °C for lithium storage property measurement in a voltage range from 3.0 V to 5 mV at a constant current density of 50 mA g^{-1}. The lithium storage properties of NiO/MWCNT composites are shown in Fig. 5. Fig. 5(a) shows the discharge/charge curves of sample annealed at 300 °C for 1 h. During the first cycle, the initial discharge and charge capacities are 1083.8 and 720.2 mAh g^{-1}, respectively; the Coulomb's efficiency are only 66.45%. As it shown in the initial discharge curve, the voltage decreases sharply from 3.0 to 1.25 V and a plateau region appears at about 0.75 V with a capacity of 750 mAh g^{-1}. This corresponds to 2.09 Li per NiO sample considering the NiO/MWCNT composites as pure NiO. The initial discharge capacity corresponds to 3.02 Li per NiO. This is larger than the theoretical value of 2 Li per NiO ($NiO + 2Li^+ + 2e^- \rightleftharpoons Li_2O + Ni$). The discharge capacities are 763.3, 734.6, 813.5 and 861.4 mAh g^{-1} at 2nd, 10th, 20th and 30th cycles, respectively, as shown in Fig. 5(a). Fig. 5(b) shows the discharge capacity profiles vs. cycle numbers of NiO/MWCNT composites at a constant current density of 50 mA g^{-1}. For sample annealed at 300 °C, we can see that the discharge capacities are kept stable at ~800 mAh g^{-1} and the coulombic efficiency maintains about 97% after 50 discharge/charge cycles. For the sample of 250 °C/4 h, the discharge capacity stabilize at 500–580 mAh g^{-1} in the early 25 cycles (Fig. 5(b)). However, after 25 cycles, the capacity decreases sharply in the subsequent cycles (Fig. 5(b), black curve). The sample annealed at 300 °C has better lithium storage properties due to good crystallinity and better contact between NiO and MWCNTs compared to the sample at 250 °C for 4 h. For sample annealed at 400 °C (Fig. 5(b), black curve), the initial discharge capacity is 1304.2 mAh g^{-1} which corresponds to 3.64 Li per NiO sample. It is higher than that of the samples for NiO/MWCNT composites annealed at 250 and 300 °C. The discharge capacities remain stable at ~950 mAh g^{-1} from 2nd to 5th cycles. However, after five cycles, the capacity loss increases sharply with capacity loss about 50–100 mAh g^{-1} per cycle due to the pulverization and loss of electrical contact with the current collectors. The discharge capacity is only 173.6 mAh g^{-1} at 20th cycle and capacity retention decreases to 13.3% of the initial value. These results are similar to the nanosheet-based NiO microspheres [40]. These can attribute that there are no MWCNTs in the products when the sample annealed at 400 °C as it shown in the TG and XRD curves. The NiO/MWCNT composites show superior lithium storage properties due to the synergistic effect between MWCNTs and NiO nanoparticles. MWCNTs restrict the volume expansion/contraction effects and enhance the conductivity of the composites due to the superior mechanical and electrical properties, leading to the superior lithium storage properties for NiO/MWCNT composites.

4. Conclusions

In summary, we developed a facile direct thermal decomposition method to prepare NiO/MWCNTs nanocomposites. The as-synthesized NiO/MWCNT composites after annealed at 300 °C for 1 h are well crystallized and exhibit superior properties as electrode materials for lithium ion batteries. The lithium storage properties could maintain at ~800 mAh g^{-1} after 50 discharge/charge cycles. It is much higher than the reported data of NiO and its composites. Therefore, NiO/MWCNT composites will be potential electrode material for lithium ion batteries.

Acknowledgements

This work is supported by the National Nature Science Foundation of China (No. 50972153) and Shanghai Talents Program Foundation.

References

[1] D. Eder, Chem. Rev. 110 (2010) 1348–1385.
[2] L.S. Zhang, L.Y. Jiang, C.Q. Chen, W. Li, W.G. Song, Y.G. Guo, Chem. Mater. 22 (2010) 414–419.
[3] F.F. Cao, Y.G. Guo, S.F. Zheng, X.L. Wu, L.Y. Jiang, R.R. Bi, L.J. Wan, J. Maier, Chem. Mater. 22 (2010) 1908–1914.
[4] V. Subramanian, H.W. Zhu, B.Q. Wei, Electrochem. Commun. 8 (2006) 827–832.
[5] J.S. Ye, H.F. Cui, X. Liu, T.M. Lim, W.D. Zhang, F.S. Sheu, Small 1 (2005) 560–565.
[6] R.R. Bi, X.L. Wu, F.F. Cao, L.Y. Jiang, Y.G. Guo, L.J. Wan, J. Phys. Chem. C 114 (2010) 2448–2451.
[7] H.X. Zhang, C. Feng, Y.C. Zhai, K.L. Jiang, Q.Q. Li, S.S. Fan, Adv. Mater. 21 (2009) 2299–2304.

[8] X.F. Xie, L. Gao, Carbon 45 (2007) 2365–2373.
[9] H. Zhang, G.P. Cao, Z.Y. Wang, Y.S. Yang, Z.J. Shi, Z.N. Gu, Nano Lett. 8 (2008) 2664–2668.
[10] Y.J. Chen, C.L. Zhu, T.H. Wang, Nanotechnology 17 (2006) 3012–3017.
[11] Z.H. Wen, Q. Wang, Q. Zhang, J.H. Li, Adv. Funct. Mater. 17 (2007) 2772–2778.
[12] Y.J. Chen, C.L. Zhu, X.Y. Xue, X.L. Shi, M.S. Cao, Appl. Phys. Lett. 92 (2008).
[13] H.T. Pu, F.J. Jiang, Nanotechnology 16 (2005) 1486–1489.
[14] L.S. Xu, X.H. Chen, W.Y. Pan, W.H. Li, Z. Yang, Y.X. Pu, Nanotechnology 18 (2007).
[15] Y. He, L. Huang, J.S. Cai, X.M. Zheng, S.G. Sun, Electrochim. Acta 55 (2010) 1140–1144.
[16] C.H. Xu, J. Sun, L. Gao, J. Phys. Chem. C 113 (2009) 20509–20513.
[17] J.E. Riggs, Z.X. Guo, D.L. Carroll, Y.P. Sun, J. Am. Chem. Soc. 122 (2000) 5879–5880.
[18] C.H. Xue, M.M. Shi, Q.X. Yan, Z. Shao, Y. Gao, G. Wu, X.B. Zhang, Y. Yang, H.Z. Chen, M. Wang, Nanotechnology 19 (2008).
[19] J. Park, E. Kang, S.U. Son, H.M. Park, M.K. Lee, J. Kim, K.W. Kim, H.J. Noh, J.H. Park, C.J. Bae, J.G. Park, T. Hyeon, Adv. Mater. 17 (2005) 429–434.
[20] L. Li, E.A. Gibson, P. Qin, G. Boschloo, M. Gorlov, A. Hagfeldt, L.C. Sun, Adv. Mater. 22 (2010) 1759–1762.
[21] P. Qin, M. Linder, T. Brinck, G. Boschloo, A. Hagfeldt, L.C. Sun, Adv. Mater. 21 (2009) 2993–2996.
[22] C.C. Yu, L.X. Zhang, J.L. Shi, J.J. Zhao, J.H. Gao, D.S. Yan, Adv. Funct. Mater. 18 (2008) 1544–1554.
[23] H. Pang, Q.Y. Lu, Y.C. Lia, F. Gao, Chem. Commun. (2009) 7542–7544.
[24] S. Hosogai, H. Tsutsumi, J. Power Sources 194 (2009) 1213–1217.
[25] J.Y. Lee, K. Liang, K.H. An, Y.H. Lee, Synth. Met. 150 (2005) 153–157.
[26] J.W. Lang, L.B. Kong, W.J. Wu, Y.C. Luo, L. Kang, Chem. Commun. (2008) 4213–4215.
[27] X. Wang, L. Li, Y.G. Zhang, S.T. Wang, Z.D. Zhang, L.F. Fei, Y.T. Qian, Cryst. Growth Des. 6 (2006) 2163–2165.
[28] X.H. Huang, J.P. Tu, B. Zhang, C.Q. Zhang, Y. Li, Y.F. Yuan, H.M. Wu, J. Power Sources 161 (2006) 541–544.
[29] N. Du, H. Zhang, J.X. Yu, P. Wu, C.X. Zhan, Y.F. Xu, J.Z. Wang, D.R. Yang, Chem. Mater. 21 (2009) 5264–5271.
[30] H. Qiao, N. Wu, F.L. Huang, Y.B. Cai, Q.F. Wei, Mater. Lett. 64 (2010) 1022–1024.
[31] M.M. Rahman, S.L. Chou, C. Zhong, J.Z. Wang, D. Wexler, H.K. Liu, Solid State Ionics 180 (2010) 1646–1651.
[32] Y. NuLi, P. Zhang, Z.P. Guo, D. Wexler, H.K. Liu, J. Yang, J.L. Wang, J. Nanosci. Nanotech. 9 (2009) 1951–1955.
[33] Y.N. Nuli, P. Zhang, Z.P. Guo, H.K. Liu, J. Yang, J.L. Wang, Mater. Res. Bullet. 44 (2009) 140–145.
[34] K. Matsui, B.K. Pradhan, T. Kyotani, A. Tomita, J. Phys. Chem. B 105 (2001) 5682–5688.
[35] M. Han, W.L. Zhang, C.L. Gao, Y.Y. Liang, Z. Xu, J.M. Zhu, J.H. He, Carbon 44 (2006) 211–215.
[36] B. Gao, C.Z. Yuan, L.H. Su, S.Y. Chen, X.G. Zhang, Electrochim. Acta 54 (2009) 3561–3567.
[37] Y.Z. Zheng, M.L. Zhang, P. Gao, Mater. Res. Bullet. 42 (2007) 1740–1747.
[38] H.W. Lu, D. Li, K. Sun, Y.S. Li, Z.W. Fu, Solid State Sci. 11 (2009) 982–987.
[39] D.S. Wang, T. Xie, Q. Peng, S.Y. Zhang, J. Chen, Y.D. Li, Chem. Eur. J. 14 (2008) 2507–2513.
[40] L. Liu, Y. Li, S.M. Yuan, M. Ge, M.M. Ren, C.S. Sun, Z. Zhou, J. Phys. Chem. C 114 (2010) 251–255.